Progress In Electromagnetics Research, Vol. 144, 33–43, 2014

Induced Voltage on the Overhead Line at Oil Exploiting Port under Lightning Strike

Xin Meng[1, 2, *], Bi-Hua Zhou[1], and Bo Yang[1]

Abstract—In this paper, a computational model is established for the finite-difference time-domain analyses of induced voltage on the overhead line at oil exploiting port under lightning strike. The MTLL approximate formulation is used to simulate the lightning strike, and convolutional perfectly matched layers are used to truncate the computational domain. A two-step method is established to calculate the coupling to the overhead lines to reduce the huge computational domain of the conventional 3-D FDTD simulation. Parallel implementation is introduced for the second-step calculation to overcome the memory storage limit of a single computer. With this model, the electromagnetic field at the adjacent areas and the induced voltage on the overhead line are studied when lightning strikes an oil derrick. It is demonstrated that the electromagnetic field decreases as the distance from the oil derrick increases, but the vertical field decrease much slower than the horizontal field. It is also shown that the transversely located overhead line will introduce lower voltage than the radially located line. As the length of the overhead line increases, the induced voltage increases and the low-frequency induction is strengthened. The overhead line should be set as low as possible to reduce the induced voltage.

1. INTRODUCTION

Lightning-induced voltage on lines has drawn worldwide concern from lightning researchers for years [1–9]. Many works have concentrated on the lightning-induced voltage, mainly on the induced voltage to the transmission lines [10], which is always tens of thousands kilometers long. At the oil exploiting port, a high derrick is located, which is frequently connected to the lightning channel. Also there will be huge number of overhead lines of dozens of meters long at the exploiting port, which will induce voltage when lightning strikes the oil derrick. Thus it is necessary to analyze the induced voltage on overhead lines at the oil exploiting port under lightning strike.

To simulate the lightning strike to the oil derrick, both frequency domain and time domain methods can be used. When frequency domain method is involved, the lightning channel above the ground is always regarded as a vertical electric dipole. The Sommerfeld convolution integral is introduced, but it is difficult to carry out the integral numerically [11–16].

The finite-difference time-domain (FDTD) method [17–25], which provides a simple and efficient way of solving Maxwell' equations for a variety of problems, has been widely applied in solving many types of electromagnetic problems. The FDTD method has been widely used to investigate the lightning protection since 1994 [26, 27]. A significant restrict of the FDTD method usage is that huge computational resources are expended for modeling a large problem.

In this paper, we first established a computational model for the FDTD method to study the induced voltage on the overhead line at oil exploiting port under lightning strike. The MTLL approximate formulation is used to simulate the lightning current in the lightning channel [28] when striking the oil

Received 6 November 2013, Accepted 10 December 2013, Scheduled 13 December 2013

* Corresponding author: Xin Meng (mengxing197655@126.com).

[1] National Key Laboratory on Electromagnetic Environment and Electro-Optical Engineering, PLA University of Science and Technology, Nanjing, Jiangsu 210007, China. [2] Institute of Meteorology and Oceanography, PLA University of Science and Technology, Nanjing, Jiangsu 210007, China.

derrick. The absorption performance of the usually used absorbing boundary conditions analyzed [29–33], and it is found that the convolutional perfectly matched layer (CPML) [33] is the most effective for this problem. A two-step method is introduced to calculate the induced voltage on the overhead lines in order to reduce the computational domain of a conventional 3D-FDTD simulation of the whole domain. Parallel FDTD implementation is used to overcome the memory storage limit of a single computer when calculating the second-step simulation [34, 35].

With the proposed FDTD calculation model, the electromagnetic field at the adjacent area is analyzed when lightning strikes the oil derrick, and then the induced voltage on the overhead line is studied. It is demonstrated that the transversely located overhead line will introduce lower induced voltage than the radially located line. As the line length increases, the induced voltage increases and the low-frequency induction is strengthened. Additionally, the overhead line should be set as low as possible to reduce the induced voltage.

2. THE DIRECT LIGHTNING STRIKE MODEL

A homogenous ground is considered in this paper, and it is assumed that ground has constant dielectric parameters. The relative permittivity of ground is set at $\varepsilon_r = 10.0$, and the conductivity is $\sigma_g = 0.02\,\mathrm{S/m}$.

In this section, the calculation model for the FDTD analysis of the induced voltage on the overhead line when lightning strikes an oil derrick. First, the model of lightning strike to an oil derrick is introduced, and then absorbing boundary conditions are chosen to truncate the computational domain. Third, a two-step method is introduced to calculate the voltage induced on the overhead lines to reduce the huge computational domain usage of the ordinary 3-D FDFD simulation. Finally, parallel implementation is introduced to overcome the memory limit of the serial FDTD when carrying out the second-step calculation.

2.1. Modeling of Lightning Strike to an Oil Derrick

There are many models to simulate the lightning strike [28, 36–41], and here the modified transmission-line linear (MTLL) model [28] is used to simulate the lightning strike. The calculation model of lightning strike to an oil derrick is as shown in Fig. 1, where the height of the oil derrick is h, ρ_{bot} the current reflection coefficient at the bottom of the tall object, and ρ_{top} the current reflection coefficient at the top of the object for upward-propagating waves. The coefficients ρ_{bot} and ρ_{top} can be obtained from

$$\rho_{top} = \frac{Z_{ob} - Z_{ch}}{Z_{ob} + Z_{ch}} \tag{1}$$

$$\rho_{bot} = \frac{Z_{ob} - Z_{gr}}{Z_{ob} + Z_{gr}} \tag{2}$$

where Z_{ob} is the characteristic impedance of the strike object, Z_{ch} the equivalent impedance of the lightning channel, and Z_{gr} the grounding impedance. The height of the oil derrick is $h = 55\,\mathrm{m}$, and it is

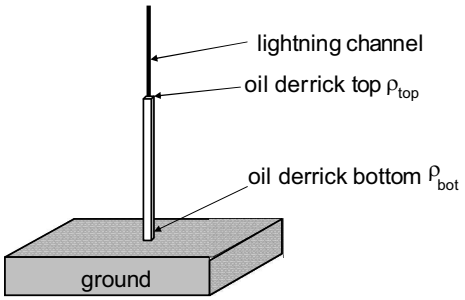

Figure 1. The model of lightning strike to an oil derrick.

chosen that $Z_{ob} = 300\,\Omega$, $Z_{ch} = 900\,\Omega$, and $Z_{gr} = 300\,\Omega$, and then it can be obtained that $\rho_{top} = -0.5$ and $\rho_{bot} = 1.0$ in this paper [36].

For the case of lightning strike to a tall object, the equation for current along the oil derrick can be written as

$$I(z',t) = \frac{1-\rho_{top}}{2} \times \sum_{n=0}^{\infty} \left[\rho_{bot}^{n} \rho_{top}^{n} I_{sc}\left(h, t - \frac{h-z'}{c} - \frac{2nh}{c}\right) + \rho_{bot}^{n+1} \rho_{top}^{n} I_{sc}\left(h, t - \frac{h+z'}{c} - \frac{2nh}{c}\right)\right] \quad \text{for } 0 \le z \le h \text{ (along the oil derrick)} \tag{3}$$

The equation for current along the lightning channel can be written as

$$I(z',t) = \frac{1-\rho_{top}}{2} \times \left[I_{sc}\left(h, t - \frac{z'-h}{v}\right) + \sum_{n=1}^{\infty} \rho_{bot}^{n} \rho_{top}^{n} I_{sc}\left(h, t - \frac{z'-h}{c} - \frac{2nh}{c}\right)\right] \quad \text{for } z \ge h \text{ (along the lightning channel)} \tag{4}$$

where n is an index representing the successive multiple reflections occurring at the two ends of the oil derrick, c the speed of light in free space, and v the return strike wave front speed. It is chosen that $v = c/3$ when $z' > h$, and $v = c$ when $z' < h$. In this paper, the calculated lightning channel is 1000 m high. $I(z',\, t)$ is the channel current of the height z' at the time t (which is defined as the lightning current that will be measured at an ideally grounded strike object of negligible height), which can be given by

$$I_{sc} = 1.1 \times I_0 \times \left(e^{-\alpha t} - e^{-\beta t}\right) \tag{5}$$

here $I_0 = 100\,\text{kA}$, $\alpha = 9.2 \times 10^3$ and $\beta = 0.8 \times 10^7$ in this paper.

2.2. Selection of the Absorbing Boundary Conditions

To truncate the computational domain, an absorbing boundary condition (ABC) is need [29–33]. In the numerical calculation, the Mur ABC [29] and the Liao's extrapolation ABC [30] are widely used for its ease of implementation. However, numerical experiments have shown that the Liao's ABC introduces much less reflection than the Mur ABC, with little sensitivity to the wave-propagation angle or to numerical phase-velocity variations.

The perfectly matched layer (PML) [31] is always used to truncate the computational domain, but it suffers from late-time reflection when terminating highly elongated lattices or when simulating fields with very long time signatures. However, the Modified PML (MPML) [32] has been proved to be more efficient at absorbing the transient waves than the PML. Additionally, the convolution PML (CPML) [33] is highly absorptive of evanescent modes.

In this part, the CPML performance is compared with the Liao's ABC and MPML to choose the best ABC for the lightning strike to an oil derrick analyses. To this point, a two dimensional simulation of the problem shown in Fig. 1 is performed, and the reflection error is computed by

$$R_{\text{dB}} = 20 \log_{10} \frac{\left|\psi_x^{ref}(t) - \psi_x^{T}(t)\right|}{\max\left|\psi_x^{ref}(t)\right|} \tag{6}$$

where $\psi_x^T(t)$ represents the field computed in the test domain, and $\psi_x^{ref}(t)$ is the reference field computed using the large domain where no reflection is reached.

The reflection error brought about by the Liao's ABC, MPML and CPML are graphed in Fig. 2. It can be seen that the CPML performance is superior to Liao's ABC and MPML, and the late-time reflection error introduced by the CPML is much smaller than the Liao's ABC and MPML. Furthermore, the CPML can provide significant memory savings when computing the wave interaction of elongated structures compared with MPML. Therefore, in the following analysis, an 8-cell-thick CPML is used to truncate the computational domain.

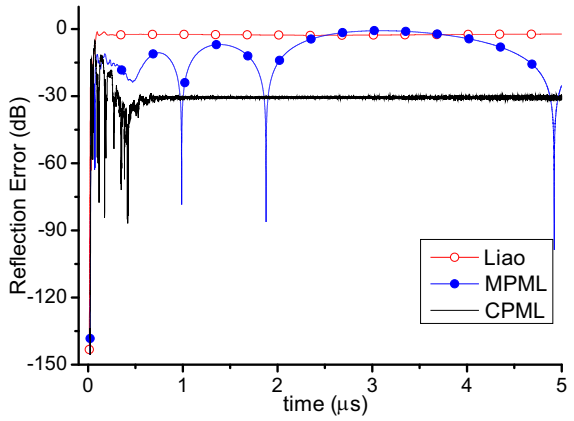

Figure 2. Reflection error of the electric field intensity relative to the field's transient amplitude versus time.

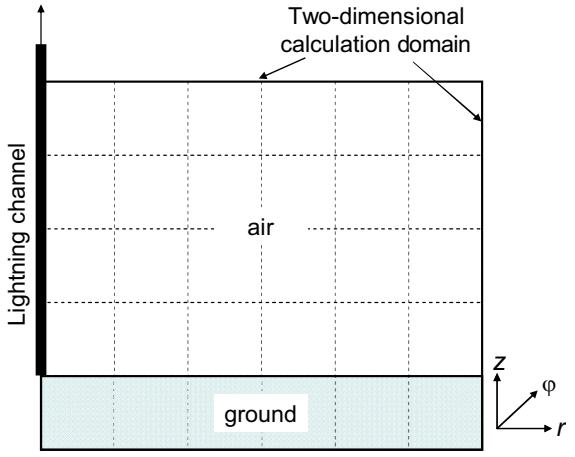

Figure 3. The 2-D cylindrical coordinate FDTD computational domain of the first step.

2.3. Two-Step Method to Calculate the Transmission Line Coupling

To calculate the induced voltage on the overhead line at the oil exploiting port when lightning strikes the oil derrick, two steps calculation are carried out. At the first step, a 2-D cylindrical coordinate FDTD simulation is carried out to get the radiated electromagnetic field near the oil derrick. Then a 3-D FDTD simulation is carried out to calculate the induced voltage on the overhead line.

The 2-D cylindrical coordinate FDTD calculation domain of the first step is as shown in Fig. 3, and the Maxwell equations are solved by the following FDTD updating equations [17]

$$E_r^{n+1}\left(i+\frac{1}{2},k\right)=\frac{2\varepsilon_r\varepsilon_0-\sigma_g\Delta t}{2\varepsilon_r\varepsilon_0+\sigma_g\Delta t}E_r^{n}\left(i+\frac{1}{2},k\right)-\frac{2\Delta t}{2\varepsilon_r\varepsilon_0+\sigma_g\Delta t}\left\{\frac{H_\varphi^{n+\frac{1}{2}}\left(i+\frac{1}{2},k+\frac{1}{2}\right)-H_\varphi^{n+\frac{1}{2}}\left(i+\frac{1}{2},k-\frac{1}{2}\right)H_\phi\Big|}{\Delta z}\right\} \tag{7}$$

$$E_z^{n+1}\left(i,k+\frac{1}{2}\right)=\frac{2\varepsilon_r\varepsilon_0-\sigma_g\Delta t}{2\varepsilon_r\varepsilon_0+\sigma_g\Delta t}E_z^{n}\left(i,k+\frac{1}{2}\right)+\frac{2\Delta t}{2\varepsilon_r\varepsilon_0+\sigma_g\Delta t}\frac{1}{i\Delta r}\left\{\left(i+\frac{1}{2}\right)H_\varphi^{n+\frac{1}{2}}\left(i+\frac{1}{2},k+\tfrac{1}{2}\right)-\left(i-\frac{1}{2}\right)H_\varphi^{n+\frac{1}{2}}\left(i-\frac{1}{2},k+\frac{1}{2}\right)\right\} \tag{8}$$

$$H_\varphi^{n+\frac{1}{2}}\left(i+\frac{1}{2},k+\tfrac{1}{2}\right)=H_\varphi^{n\frac{1}{2}}\left(i+\tfrac{1}{2},k+\tfrac{1}{2}\right)-\frac{\Delta t}{\mu_0}\left\{\frac{E_r^{n+1}\left(i+\frac{1}{2},k+1\right)-E_r^{n+1}\left(i+\frac{1}{2},k\right)}{\Delta z}-\frac{E_z^{n+1}\left(i+1,k+\frac{1}{2}\right)-E_z^{n+1}\left(i,k+\frac{1}{2}\right)}{\Delta r}\right\} \tag{9}$$

The second calculation step is a 3-D FDTD domain simulation elongated along the overhead line direction, which is to calculate the induced voltage on the overhead line. At this step, the lightning radiated electromagnetic field, which is calculated at the first step, is introduced through the total-field/scattered-field boundary [17] as the source. The calculation domain of the 3-D simulation is as shown in Fig. 4, where in Fig. 4(a) the overhead horizontal line is transversely located while the overhead horizontal line is radially located in Fig. 4(b).

To validate the efficiency of the proposed two-step method, a reference benchmark is needed. In this paper, the results calculated from the ordinary 3D-FDTD simulation of the whole computational

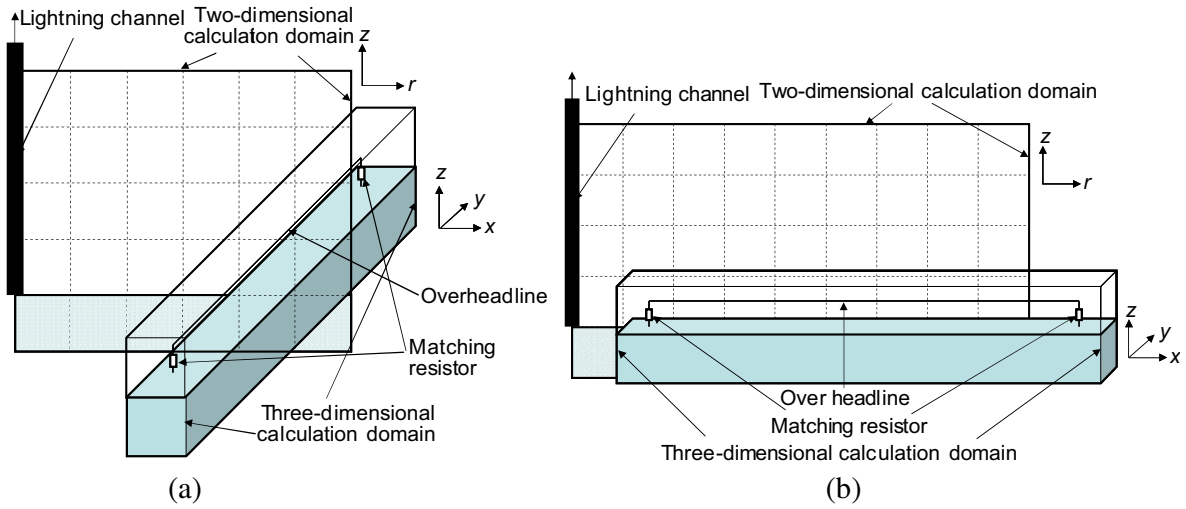

Figure 4. The 3-D calculation domain of the second step to calculate the induced voltage on overhead lines, where the calculation domain of the first step is also graphed. (a) The overhead line is transversely located. (b) The overhead line is radially located.

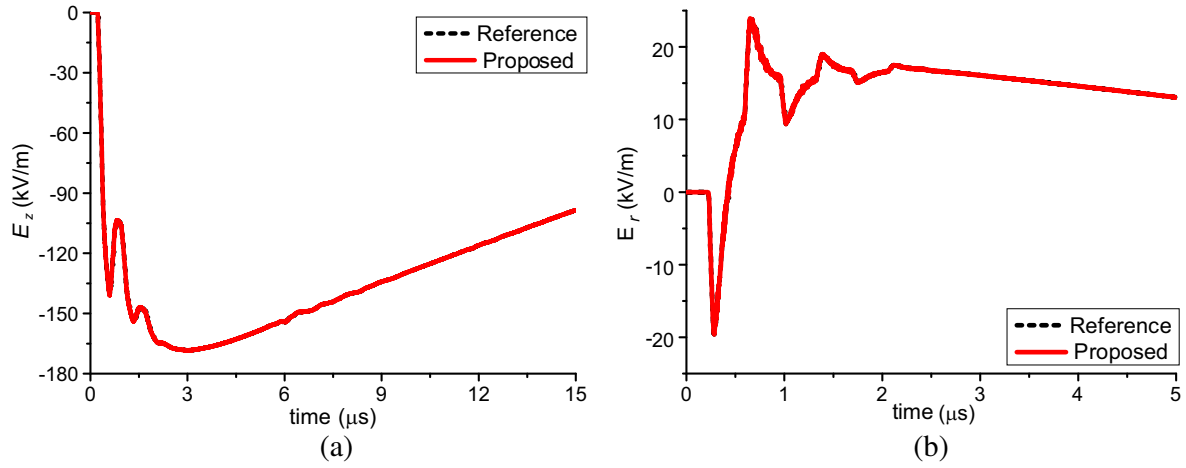

Figure 5. The horizontal and vertical electric field, which are 10 m high from the ground and 50 m away from the oil derrick, as obtained from the proposed method and the 3D-FDTD method. (a) The horizontal electric field. (b) The vertical electric field.

domain are used to provide a benchmark for comparison.

Figure 5 graphs both the horizontal and vertical electric fields obtained from the proposed method and the ordinary 3D-FDTD method. It can be seen that the electric field calculated from the proposed method is in good agreement with that obtained from the 3D-FDTD method, which demonstrates the accuracy of the proposed method.

If an ordinary 3-D simulation is performed, a 70 m × 70 m × 1010 m domain will be involved for the case that the lightning channel is 1000 m high, overhead line 50 m in length, and 50 m from the oil derrick. However, only a 20 m × 70 m × 20 m domain is used with the proposed method, which means that the computational domain of the proposed method is only about 1/176 of the ordinary 3-D FDTD simulation. It can also be demonstrated that as the distance of the involved area to the oil derrick increases, there will be much more significant computational resource of the proposed method. Thus the efficiency of the proposed method is validated.

2.4. Parallel Implementation of the Second Step

Parallel FDTD is a kind of algorithm that the computational domain is divided into several sub-domains and each node only handle for the corresponding sub-domain calculation [34, 35]. Therefore, the requirement of the computational storage and time is reduced several times.

The computational domain of the second step calculation is a highly elongated structure, thus a one-dimensional division will be efficient. The computational space is divided into several parts, and the grid division and fields' interaction of neighbor nodes, node N and node $N+1$, are shown in Fig. 6, where Fig. 6(a) is for the transversely located overhead line while Fig. 6(b) is for the radially located overhead line.

To approve the efficiency of the proposed parallel implementation program, the calculated electric field by the parallel FDTD simulation is compared with that given by the serial FDTD simulation. The problem of Fig. 2(b) is computed, and the calculated E_z field which is 200 m from the oil derrick is graphed in Fig. 7, where the parallel FDTD is implemented on 4 PC nodes. It can be seen that the parallel FDTD gives the same result as the serial FDTD, thus the efficiency of the parallel strategy adopted here is verified. The computer memory and time usage of the proposed parallel program is 30% and 33% respectively compared with the serial FDTD simulation.

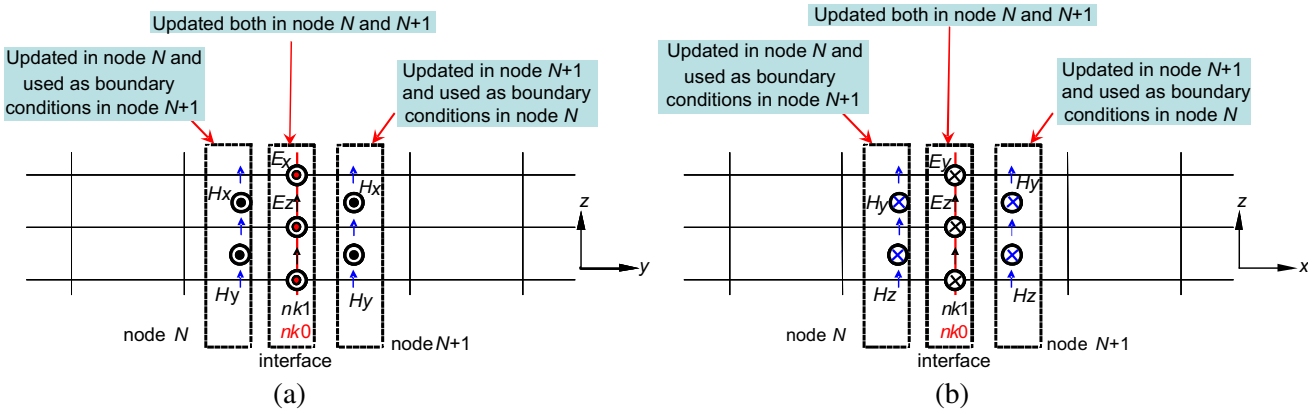

Figure 6. Configuration of field component exchange. (a) The parallel program for the transversely located overhead line. (b) The parallel program for the radially located overhead line.

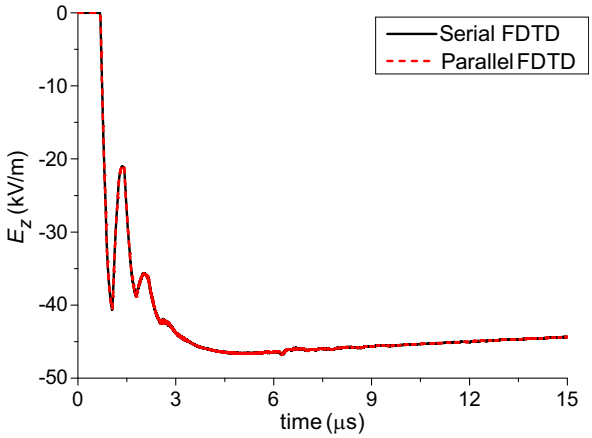

Figure 7. Comparison of the vertical electric field 200 m from the oil derrick between parallel implementation and serial FDTD.

3. INDUCED VOLTAGE ON THE OVERHEAD LINE

In this section, the induced voltage on the overhead lines, which are transversely and radially located as shown in Figs. 2(a) and 2(b), are studied when lightning strikes the oil derrick.

First, both the vertical and horizontal electric fields are monitored as the distance from the lightning struck oil derrick increases. Then the induced voltage on the transversely and radially located overhead lines is studied. Third, the overhead line length effect on the induced voltage is analyzed. Fourth, the height of the overhead line is varied and the induced voltage is calculated.

3.1. The Electromagnetic Field near the Oil Derrick

To analyze the induced voltage on the overhead line, the electric field near the oil derrick is monitored firstly. Fig. 8(a) graphs the horizontal electric field 10 m from the ground at varied distances from the oil derrick, it can be seen that the horizontal electric field decreases dramatically as the distance increases. It can also be demonstrated that the horizontal electric field near the lightning struck oil derrick is decreased in a $1/r$ variation, where r is the distance from the oil derrick.

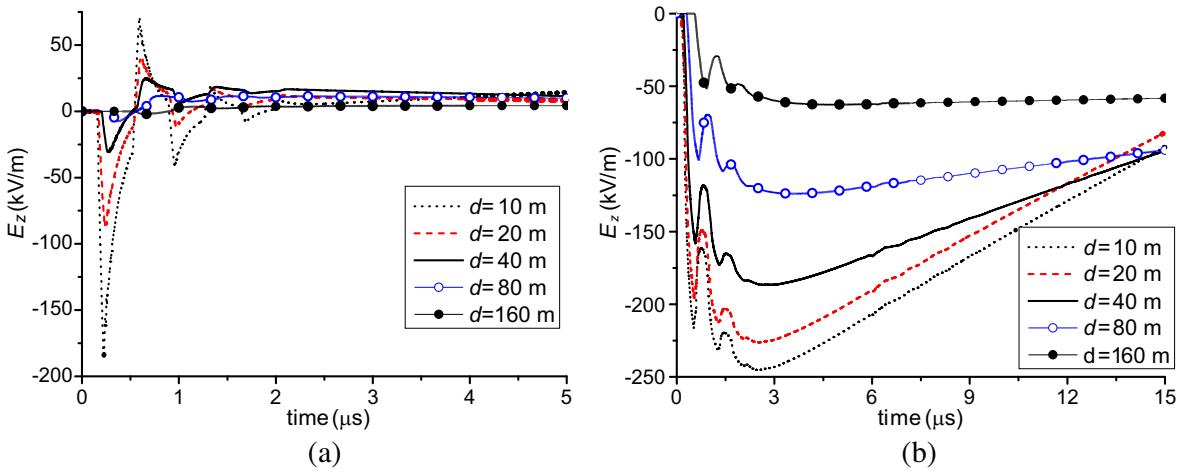

Figure 8. The horizontal and vertical electric field 10 m high from the ground. (a) The horizontal electric field. (b) The vertical electric field.

In Fig. 8(b) is plotted the vertical electric field, and it is clear that the vertical electric field decreases as the distance from the oil derrick increases. The peak vertical electric field value is -245 V/m when $d = 10$ m while -225 V/m when $d = 20$ m, which means that the vertical electric field is not decreased in a $1/r$ variation.

From comparison of Figs. 8(b) and 8(a), it can also be concluded that not only the vertical electric field is larger than the horizontal field but also the duration of the vertical field is much longer than that of the horizontal field. It can also been seen that the vertical electric field decreases much slower than the horizontal electric field.

3.2. The Overhead Line Direction Effect on the Induced Voltage

The overhead line is set transversely and radially to the oil derrick, and the induced voltage is calculated. To this point, the length of the overhead line is 20 m, and they are set to be 2 m from the ground. The distance between the oil derrick and the center of the transverse line is 5 m, and the same distance is set from the oil derrick to the adjacent side of the radially located line. The induced voltages both at the adjacent side and far side on the radially set line are graphed in Fig. 9, where the transverse line induced voltage is also included.

It is clear that the induced voltage of the radially located line at the side adjacent to the oil derrick is much higher than that at the far side. It can also be seen from Fig. 9 that the induced voltage on

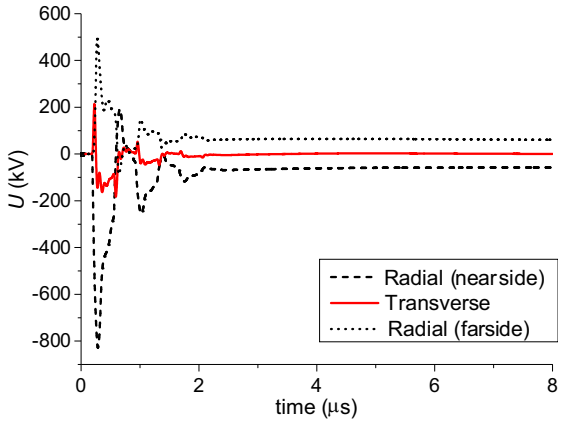

Figure 9. The induced voltage on the transversely and radially located overhead line, where – – – indicate the induced voltage on the radially located line at the side and . . . . . indicates that at the far side.

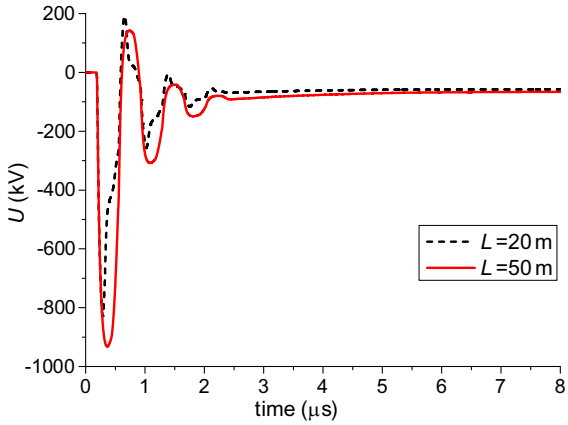

Figure 10. The induced voltage when the overhead line length is 20 m and 50 m respectively.

the transversely located overhead line is quite smaller than the voltage at the near side of the radially located line, and even smaller than that at the far side of the radial line. Thus it can be concluded that the transversely located overhead line will introduce lower voltage than the radially located overhead line.

3.3. The Line Length on the Induced Voltage

The length of the radially located overhead line is varied from $L = 20\,\text{m}$ to 50 m, and the induced voltage is studied. The near side of the line is 5 m from the oil derrick, and the line is 2 m in height. In Fig. 10 is graphed the induced voltage of the line when the line length is 20 m and 50 m respectively.

It can be seen from Fig. 10 that the peak value of the induced voltage is increased from 820 kV to 930 kV as the overhead line length is varied from 20 m to 50 m. It can also be seen that the waveform of the induced voltage is becomes smoothly as the length is increased from 20 m to 50 m, which denotes that the low-frequency induction on the line is strengthened as the overhead line length is increased.

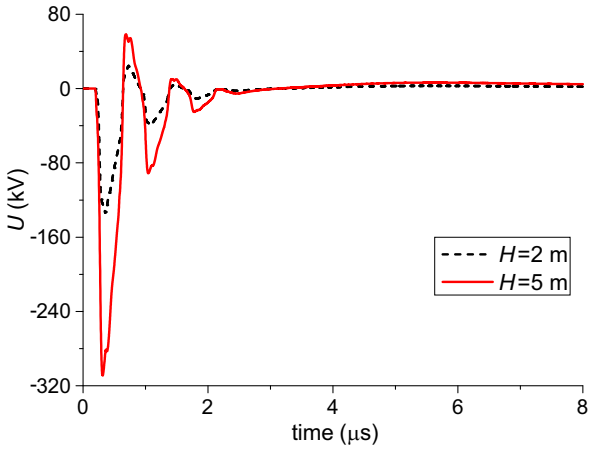

Figure 11. The induced voltage when the overhead line is 2 m and 5 m high from the ground respectively.

3.4. The Line Height Effect on the Induced Voltage

The overhead line height effect on the induced voltage is studied in this part. To this point, the induced voltage on a transversely located overhead line, which is 20 m in length and 20 m from the oil derrick, is simulated. The overhead line is 20 m in length, and the height of the line is varied from 2 m to 5 m. The induced voltage is calculated and graphed in Fig. 11.

It can be seen from Fig. 11 that the peak value of the induced voltage is increased dramatically from 134 kV to 308 kV, which means that the vertical line will introduce huge induced voltage to the line. Thus it is better to set the overhead line as low as possible to reduce the induced voltage.

From the analyses in this part, it can be concluded that the value and duration of the vertical field is much longer than that of the horizontal field, and the vertical electric field decreases much slower as the distance from the oil derrick increases. It can also be concluded that the transversely located overhead line will introduce lower voltage than the radially located line. As the overhead line length increases, the induced voltage increases and the low-frequency induction is strengthened. High overhead line will introduce a much higher voltage, thus the overhead line should be set as low as possible to reduce the induced voltage.

4. CONCLUSIONS

In this work, a new model has been established for the FDTD analysis of the induced voltage on the overhead lines at the oil derrick port. The MTLL approximate formulation is used to simulate the lightning strike to an oil derrick, and the CPML is chosen among the absorbing boundary conditions to truncate the computational domain. Third, a two-step method is introduced to calculate the voltage induced on the overhead line in order to reduce the computational resources. Finally, parallel implementation is introduced in the second-step calculation to overcome the memory limit of the serial FDTD.

With the proposed FDTD calculation model, the electromagnetic field near the oil derrick is analyzed when lightning strikes the oil derrick firstly, and then the voltage induced on the overhead line is studied as the overhead line position is varied. It can be seen that the electromagnetic field decreases as the distance from the oil derrick increases, but the vertical field decreases much slower than the horizontal field. It is shown that the transversely located overhead line will introduce lower voltage than the radially located line, thus it is better to set the line transverse rather than radial. As the line length increases, the induced voltage increases and the low-frequency induction strengthened. It is also demonstrated that high overhead line will result in a much higher induced voltage, and the overhead line should be set as low as possible to reduce the induced voltage.

The proposed model is capable of analysing the induced voltage of other equipments when lightning strikes an oil derrick, and the conclusions derived in this paper will be useful in the line setting design at the oil derrick port.

ACKNOWLEDGMENT

This work was supported by the National Natural Science Foundation of China under Grant No. 41305017.

REFERENCES

1. IEC 62305-3, *Protection Against Lightning — Part 3: Physical Damage to Structures and Life Hazard*, 1st Edition, 2006.
2. Master, M. J. and M. A. Uman, "Lightning-induced voltage on power line: Theory," *IEEE Trans. on Power, Apparatus, Syst.*, Vol. 103, 2502–2518, Sep. 1984.
3. Diendorfer, G. and M. A. Uman, "An improved return stroke model with specified channel-base current," *J. Geophys. Res.*, Vol. 95, No. 13, 13621–13644, 1990.

4. Cooray, V. and F. de la Rosa, "Shapes and amplitudes of the initial peaks of lightning-induced voltage in power lines over finitely conducting earth: Theory and comparison with experiment," *IEEE Trans. on Antennas and Propagat.*, Vol. 34, 88–92, Jan. 1986.
5. Izadi, M., M. Z. A. Ab Kadir, and C. Gomes, "Evaluation of electromagnetic fields associated with inclined lightning channel using second order FDTD-Hybrid Methods," *Progress In Electromagnetics Research*, Vol. 117, 209–236, 2011.
6. Izadi, M., M. Z. A. Ab Kadir, C. Gomes, V. Cooray, and J. Schoene, "Evaluation of lightning current and velocity profiles along lightning channel using measured magnetic flux density," *Progress In Electromagnetics Research*, Vol. 130, 473–492, 2012.
7. Izadi, M., M. Z. A. Ab Kadir, C. Gomes, and V. Cooray, "Evaluation of lightning return stroke current using measured electromagnetic fields," *Progress In Electromagnetics Research*, Vol. 130, 581–600, 2012.
8. Gomes, C. and M. Z. A. A. Kadir, "Protection of naval systems against electromagnetic effects due to lightning," *Progress In Electromagnetics Research*, Vol. 113, 333–349, 2011.
9. Paolone, M., C. A. Nucci, E. Petrache, and F. Rachidi, "Mitigation of lightning-induced overvoltage in medium voltage distribution lines by means of periodical grounding of shielding overhead line and of surge arresters: Modelling and experimental validation," *IEEE Trans. on Power Del.*, Vol. 19, No. 1, 423–431, Jan. 2004.
10. Rubinstein, M., "An approximate formula for the calculation of the horizontal field from lightning at close, intermediate and long range," *IEEE Trans. on Electromagn Compat.*, Vol. 38, 531–535, 1996.
11. Cooray, V. and V. Scuka, "Lightning induced overvoltage in power lines: Validity of various approximations made in overvoltage calculations," *IEEE Trans. on Electromagn. Compat.*, Vol. 40, No. 4, 355–363, 1998.
12. Norton, K. A., "Propagation of radio waves over the surface of the earth in the upper atmosphere," *Proc. IEEE*, Vol. 25, 1203–1237, 1937.
13. Maclean, T. S. M. and Z. Wu, *Radiowave Propagation over Ground*, 1st Edition, Chapman and Hall, London, UK, 1993.
14. Cooray, V., "Horizontal fields generated by return strokes," *Radio Sci.*, Vol. 27, 529–537, Jul–Aug. 1992.
15. Cooray, V., "Underground electromagnetic fields generated by the return strokes of lightning flashes," *IEEE Trans. on Electromagn. Compat.*, Vol. 43, No. 1, 75–84, 2001.
16. Delfino, F., R. Procopio, M. Rossi, et al., "An algorithm for the exact evaluation of the underground lightning electromagnetic fields," *IEEE Trans. on Electromagn. Compat.*, Vol. 49, No. 2, 401–411, 2007.
17. Taflove, A. and S. C. Hagness, *Computational Electrodynamics: The Finite-difference Time-domain Method*, 3rd Edition, Artech House, 2005.
18. Xiong, R., B. Chen, J.-J. Han, Y.-Y. Qiu, W. Yang, and Q. Ning, "Transient resistance analysis of large grounding systems using the FDTD method," *Progress In Electromagnetic Research*, Vol. 132, 159–175, 2012.
19. Xiong, R., B. Chen, Y. Mao, B. Li, and Q.-F. Jing, "A simple local approximation FDTD model of short apertures with a finite thickness," *Progress In Electromagnetics Research*, Vol. 131, 135–152, 2012.
20. Xiong, R., B. Chen, Y.-X. Mao, and W. Yang, "Optimal programs to reduce the resistance of grounding systems," *Progress In Electromagnetics Research*, Vol. 139, 211–227, 2013.
21. Xiong, R., B. Chen, L.-H. Shi, Y.-T. Duan, and G. Zhang, "A simple method to reduce the peak transient grounding resistance value of a grounding system," *Progress In Electromagnetics Research*, Vol. 138, 255–267, 2013.
22. Lee, K. H., I. Ahmed, R. S. M. Goh, E. H. Khoo, E. P. Li, and T. G. G. Hung, "Implementation of the FDTD method based on lorentz-drude dispersive model on GPU for plasmonics applications," *Progress In Electromagnetics Research*, Vol. 116, 441–456, 2011.

23. Kong, Y.-D. and Q.-X. Chu, "Reduction of numerical dispersion of the six-stage split-step unconditional-stable FDTD method with controlling parameters," *Progress In Electromagnetics Research*, Vol. 122, 175–196, 2012.
24. Sirenko, K., V. Pazynin, Y. K. Sirenko, and H. Bağci, "An FFT-accelerated FDTD scheme with exact absorbing conditions for characterizing axially symmetric resonant structures," *Progress In Electromagnetics Research*, Vol. 111, 331–364, 2011.
25. Kong, L.-Y., J. Wang, and W.-Y. Yin, "A Novel dielectric conformal FDTD method for computing SAR distribution of the human body in a metallic cabin illuminated by an intentional electromagnetic pulse (IEMP)," *Progress In Electromagnetics Research*, Vol. 126, 355–373, 2012.
26. Morris, M. E., R. J. Fisher, G. H. Schnetzer, K. O. Merewether, and R. E. Jorgenson, "Rocket-triggered lightning studies for the protection of critical assets," *IEEE Transactions on Industry Applications*, Vol. 30, No. 3 355–373, 1994.
27. Rachidi, F., C. A. Nucci, and M. Ianoz, "Transient analysis of multiconductor lines above a lossy ground," *IEEE Trans. on Power Del.*, Vol. 14, No. 1, 294–302, 1999.
28. Rakov, V. A. and A. A. Dulzon, "Calculated electromagnetic fields of lightning return stroke," *Tekh. Elektrodianm.*,Vol. 1, 87–89, 1987.
29. Mur, G., "Absorbing boundary conditions for the finite-difference approximation of the time-domain electromagnetic field equations," *IEEE Trans. on Electromagn. Compat.*, Vol. 23, 377–382, 1981.
30. Liao, Z. P., H. L. Wong, B. P. Yang, and Y. F. Yuan, "A transmitting boundary for transient wave analyses," *Scientia Sinica*, Series A, Vol. XXVII, 1063–1076, 1984.
31. Berenger, J. P., "A perfectly matched layer for the absorption of the electromagnetic waves," *J. Comput. Phys.*, 185–200, 1994.
32. Chen, B., D. G. Fang, and B. H. Zhou, "Modified berenger PML absorbing boundary condition for FDTD meshes," *IEEE Microwave and Guided Wave Letters*, Vol. 44, No. 12, 1630–1639, Nov. 1995.
33. Roden, J. A. and S. D. Gedney, "Convolution PML (CPML): An efficient FDTD implementation of the CFS-PML for arbitrary media," *Microwave and Optical Technology Lett.*, Vol. 27, 334–339, 2000.
34. Vaccari, A., A. Cala' Lesina, L. Cristoforetti, and R. Pontalti, "Parallel implementation of a 3-D subgridding FDTD algorithm for large simulation," *Progress In Electromagnetics Research*, Vol. 120, 263–292, 2011.
35. Taboada, J. M., M. G. Araujo, J. M. Bertolo, L. Landesa, F. Obelleiro, and J. L. Rodriguez, "MLFMA-FFT parallel algorithm for the solution of large-scale problems in electromagnetics," *Progress In Electromagnetics Research*, Vol. 105, 15–30, 2010.
36. Vaccari, A., A. Cala' Lesina, L. Cristoforetti, and R. Pontalti, "Parallel implementation of a 3D subgridding FDTD algorithm for large simulations," *Progress In Electromagnetics Research*, Vol. 120, 263–292, 2011.
37. Baba, Y. and V. A. Rakov, "On the use of lumped sources in lightning return stroke models," *J. Geophys Res.*, Vol. 110, D03101, 2005.
38. Uman, M. A. and D. K. McLain, "Magnetic field of the lightning return stroke," *J. Geophys. Res.*, Vol. 74, 6899–6910, 1969.
39. Nucci, C. A., C. Mazzetti, F. Rachidi, et al., "On lightning return stroke models for LEMP calculations," *Proc. 19th Int. Conf. Lightning Protection*, Graz, Austria, Apr. 1988.
40. Bruce, C. E. R. and R. H. Golde, "The lightning discharge," *J. Inst. Elect. — Pt. 2*, Vol. 88, 487–520, 1941.
41. Heidler, F., "Traveling current source model for LEMP calculation," *Proc. 6th Int. Zurich Symp. Electromagn. Compat.*, 157–162, Zurich, Switzerland, Mar. 1985.